Atmos. Chem. Phys., 14, 12291–12305, 2014
www.atmos-chem-phys.net/14/12291/2014/
doi:10.5194/acp-14-12291-2014

Atmospheric Chemistry and Physics
Open Access

Modeling of HCHO and CHOCHO at a semi-rural site in southern China during the PRIDE-PRD2006 campaign

X. Li[1,2], F. Rohrer[1], T. Brauers[1,†], A. Hofzumahaus[1], K. Lu[1,*], M. Shao[2], Y. H. Zhang[2], and A. Wahner[1]

[1]Institut für Energie- und Klimaforschung Troposphäre (IEK-8), Forschungszentrum Jülich, Jülich, Germany
[2]College of Environmental Sciences and Engineering, Peking University, Beijing, China
[†]deceased
[*]now at: College of Environmental Sciences and Engineering, Peking University, Beijing, China

Correspondence to: X. Li (x.li@fz-juelich.de) and A. Wahner (a.wahner@fz-juelich.de)

Received: 4 December 2013 – Published in Atmos. Chem. Phys. Discuss.: 17 December 2013
Revised: 25 September 2014 – Accepted: 19 October 2014 – Published: 21 November 2014

Abstract. HCHO and CHOCHO are important trace gases in the atmosphere, serving as tracers of VOC oxidations. In the past decade, high concentrations of HCHO and CHOCHO have been observed for the Pearl River Delta (PRD) region in southern China. In this study, we performed box model simulations of HCHO and CHOCHO at a semi-rural site in the PRD, focusing on understanding their sources and sinks and factors influencing the CHOCHO to HCHO ratio (R_{GF}). The model was constrained by the simultaneous measurements of trace gases and radicals. Isoprene oxidation by OH radicals is the major pathway forming HCHO, followed by degradations of alkenes, aromatics, and alkanes. The production of CHOCHO is dominated by isoprene and aromatic degradation; contributions from other NMHCs are of minor importance. Compared to the measurement results, the model predicts significant higher HCHO and CHOCHO concentrations. Sensitivity studies suggest that fresh emissions of precursor VOCs, uptake of HCHO and CHOCHO by aerosols, fast vertical transport, and uncertainties in the treatment of dry deposition all have the potential to contribute significantly to this discrepancy. Our study indicates that, in addition to chemical considerations (i.e., VOC composition, OH and NO_x levels), atmospheric physical processes (e.g., transport, dilution, deposition) make it difficult to use the CHOCHO to HCHO ratio as an indicator for the origin of air mass composition.

1 Introduction

The degradation of directly emitted volatile organic compounds (VOCs) results in the formation of ozone (O_3) and secondary organic aerosols (SOAs) in the troposphere (Finlayson-Pitts and Pitts, 2000). This process consists of the oxidation of VOCs by hydroxyl radical (OH), O_3, and nitrate radical (NO_3). Detailed understanding of the VOCs' degradation mechanism is challenged by the co-existence of vast variety of VOC species in the atmosphere. However, investigations on ubiquitous oxidation intermediates, e.g., formaldehyde (HCHO) and glyoxal (CHOCHO), can help us to test and improve the current knowledge of the VOCs' sources and degradation pathways.

HCHO is the most abundant carbonyl compound in the atmosphere. Maximum HCHO concentrations can reach 100 ppb in polluted areas whereas sub-ppb levels are found in remote areas (Finlayson-Pitts and Pitts, 2000). Most of HCHO is produced during the oxidation of organic compounds (Fortems-Cheiney et al., 2012). While methane (CH_4) oxidation by OH radicals is the major source of HCHO in remote areas, the HCHO production in regions (e.g., forest, urban area) with elevated non-methane hydrocarbons (NMHCs) (i.e., alkanes, alkenes, aromatics, isoprene, and terpenes) is dominated by their degradation. Direct emissions of HCHO originate mainly from fossil fuel combustion (Schauer et al., 1999, 2002), biomass burning (Lee et al., 1997), and vegetation (DiGangi et al., 2011), but are usually of minor importance (Parrish et al., 2012). The known removal pathways of HCHO in the atmosphere are

reaction with OH, photolysis, and dry / wet deposition. Heterogeneous uptake by cloud droplets and aerosols is speculated to be an additional sink of HCHO, which could contribute to the HCHO destruction (Zhou et al., 1996; Tie et al., 2001; Fried et al., 2003a). However, the existence of this process in the lower troposphere is still under discussion. Laboratory experiments indicate reactive loss of HCHO can happen on surfaces of H_2SO_4 aerosols (Jayne et al., 1996), mineral dust aerosols (Sassine et al., 2010), and organic aerosols (Li et al., 2011). Field observations by Wang et al. (2010) suggest an uptake of HCHO by aerosols in the presence of amines (or ammonia) and carbonyl compounds. HCHO oligomerization is also proposed to contribute to the partitioning of gaseous HCHO to aerosol phase (Toda et al., 2014). But, during a chamber study, Kroll et al. (2005) did not find any growth of both neutral ($(NH_4)_2SO_4$) and acidic (NH_4HSO_4) aerosols in the presence of gaseous HCHO, suggesting that the uptake of HCHO by aerosols is unlikely taking place. Although numerical simulations of HCHO, either by multi-dimensional models or box models, can in some cases reproduce HCHO observations (Wagner et al., 2001; Fried et al., 2003b; MacDonald et al., 2012), significant discrepancies between modeled and measured HCHO concentration have been frequently found (Choi et al., 2010; Fried et al., 2011, and references therein). The model underestimation can arise from the following: deviation from the steady-state assumption (Fried et al., 2003a), direct emissions and their transport (Fried et al., 2011), missing consideration of HCHO production from unmeasured precursors (Kormann et al., 2003; Choi et al., 2010), etc. If the steady-state assumption is disturbed, e.g., in the vicinity of fresh emissions, the model can also overpredict the measured HCHO concentration (Fried et al., 2011).

CHOCHO is the smallest dicarbonyl compound in the atmosphere. Ambient concentration of CHOCHO ranges from tens of ppt in remote and rural areas to $\approx$1 ppb in heavy polluted urban regions (e.g., Volkamer et al., 2007; Washenfelder et al., 2011; DiGangi et al., 2012). Compared to HCHO, CHOCHO has nearly no primary sources except biomass burning and biofuel combustion. Globally, isoprene and ethyne are the major precursors of CHOCHO (Fu et al., 2008). While local CHOCHO production is dominated by aromatics degradation in urban or sub-urban areas (Volkamer et al., 2007; Washenfelder et al., 2011), significant contributions from 2-methyl-3-buten-2-ol (MBO) and isoprene oxidation are identified for rural areas (Huisman et al., 2011). Removal of gaseous CHOCHO is driven by reaction with OH, photolysis, deposition, and loss on aerosol surfaces (Fu et al., 2008). By comparing CHOCHO column densities derived from a global model simulation to satellite observations, Myriokefalitakis et al. (2008) and Stavrakou et al. (2009) speculate of a missing global source of CHOCHO. Similar study performed recently by Liu et al. (2012) suggests that the missing CHOCHO sources in China is most likely due to the underestimation of aromatics in the VOC emission inventory. As first indicated by Volkamer et al. (2007), if loss of CHOCHO on aerosol surfaces is not taken into account, models can substantially overestimate measured CHOCHO concentrations. Laboratory studies found that uptake of CHOCHO by aerosols is mainly through polymerization process and is related with the acidity and the ionic strength within the aqueous phase of aerosols (Jang and Kamens, 2001; Liggio et al., 2005; Kroll et al., 2005). Once CHOCHO is taken up by aerosols, it can contribute to the formation of secondary organic aerosols (Volkamer et al., 2007; Tan et al., 2009; Washenfelder et al., 2011).

Given that HCHO and CHOCHO have similar sinks but different sources, the CHOCHO to HCHO ratio (R_{GF}) has been proposed to be a tracer of changes of VOC mixture in the atmosphere. Based on satellite observations, Vrekoussis et al. (2010) conclude that regions with R_{GF} lower than 0.045 are under influence of anthropogenic emissions, whereas R_{GF} higher than 0.045 often indicates that VOC emissions mostly originate from biogenic sources. Average R_{GF} up to 0.2–0.4 were observed by MacDonald et al. (2012) in an Asian tropic forest. However, after analyzing the measured R_{GF} and relevant trace gases at a rural site, DiGangi et al. (2012) found that higher R_{GF} corresponded to increased anthropogenic impact on local photochemistry.

The Pearl River Delta (PRD) region located in southern China has been identified by satellite observations as the region with high levels of HCHO and CHOCHO (Wittrock et al., 2006; Vrekoussis et al., 2010). Yet simultaneous ground-based measurements of HCHO and CHOCHO in this region are quite limited. During the PRIDE-PRD2006 campaign, which was dedicated to the understanding of the formation mechanism of O_3 and SOA in this heavy polluted region, we performed 1 month of continuous MAX-DOAS observations for HCHO and CHOCHO at a semi-rural site in the PRD (Li et al., 2013). The measured HCHO and CHOCHO concentrations as well as R_{GF} were as high as those obtained in other urban environments. Simultaneous measurements of HO_X ($= OH + HO_2$) radicals, trace gases, and aerosols suggest highly active photochemistry under the influence of both anthropogenic and biogenic emissions (Lou et al., 2010; Hu et al., 2012; Lu et al., 2012). In this paper, we will focus on investigating the production and destruction pathways of HCHO and CHOCHO during the PRIDE-PRD2006 campaign, and try to understand the change of R_{GF} with the change of air mass compositions.

2 Approach

2.1 Field measurements

The PRIDE-PRD2006 field campaign took place in July 2006 in the Pearl River Delta (PRD) region in southern China within the framework of the "Program of Regional Integrated Experiments of Air Quality over the Pearl River

Delta" (PRIDE-PRD2006). Field measurements of HO_X radicals, trace gases, aerosols, and meteorological parameters were performed at a semi-rural site called "Back Garden" (BG, 23.50° N, 113.03° E), which is located at the northern edge of PRD. While big cities (i.e., Zhaoqing, Foshan, Guangzhou, and Dongguan) are located tens of kilometers south of the BG site, to the north of the BG site are small towns close to mountain areas. These mountain areas are typically covered by evergreen broad-leaf forest. The BG site is next to a water reservoir and is surrounded by farmland (peanuts, lychees, trees, small forests).

Concentrations of HCHO and CHOCHO were retrieved from MAX-DOAS scattered sunlight measurements at six elevation angles. Since the concentration retrieval has been described in detail in Li et al. (2013), only a brief outline follows. During the retrieval, HCHO and CHOCHO are assumed to be well-mixed in a layer with height H. The vertical column density (VCD) and H are retrieved by comparing measured differential slant column densities (DSCDs) to those simulated by a radiative transfer model (RTM). Using the retrieved VCDs and H, mean mixing ratios of HCHO and CHOCHO in the well-mixed layer were calculated. In order to exclude the influence of clouds on the concentration retrieval, we only consider observations during cloud-free days. The errors of the retrieved HCHO and CHOCHO mixing ratios consist of statistical errors which arise mainly from the uncertainty of the measured DSCDs, and systematic errors which originate from the uncertainty of the RTM input parameters (e.g., aerosol optical depth, aerosol single scattering albedo, aerosol asymmetry factor under the Henyey–Greenstein approximation) and of the DSCD simulation. The systematic error is estimated to be around 35 %.

The MAX-DOAS measurements were performed in parallel with ground-based in situ measurements of CO, CH_4, C3–C12 NMHCs, NO_x (= NO + NO_2), O_3, aerosol physical and chemical properties, photolysis frequencies, relative humidity, and pressure on top of a hotel building (10 m a.g.l.). Simultaneously, measurements of HOx radicals, HONO, temperature, and 3d-wind were performed on top of two stacked sea containers around 20 m away from the hotel building. Details of these measurements were described in separate papers (Lu et al., 2012, and references therein). Instrumentation, time resolution, and accuracy for parameters used in this study are listed in Supplement Table S1.

2.2 Model description

Concentrations of HCHO and CHOCHO were calculated by a zero-dimensional box model using the Master Chemical Mechanism (MCM) Version 3.2 (http://mcm.leeds.ac.uk/MCM/). The model includes the full MCM chemistry for all measured NMHCs and their oxidation products. The model calculations were constrained to measurements of OH, NO, NO_2, HONO, O_3, CO, CH_4, C3–C12 NMHCs, photolysis frequencies, relative humidity, temperature, and pressure. Concentrations of ethane, ethene, and ethyne were fixed to 1.5 ppb, 3 ppb, and 1.7 ppb, respectively, estimated from few canister samples. H_2 mixing ratio was assumed to be 550 ppb. An additional loss process with a lifetime (τ_D) of 24 h was assumed for all calculated species. This lifetime corresponds to a dry deposition velocity of 1.2 cm s^{-1} and a well-mixed boundary layer height of about 1 km. The model was operated in a time-dependent mode for the entire campaign period (5–25 July), with 30 min time resolution and a 2-day spin-up time. For periods when measured NMHCs data were not available, values were taken from the campaign mean diurnal variation. With regard to missing OH values, they are estimated from the measured photolysis frequency of O_3 (J_{O1D}) using the empirical formula described by Lu et al. (2012). The model run with the above settings represents the current understanding on the HCHO and CHOCHO chemistry at the BG site, based on available precursor measurements. This base case scenario is called M0 in the text and figures. In order to investigate to which extent the model can reproduce the HCHO and CHOCHO measurements, different model scenarios were setup by including additional mechanisms in M0. Table 1 gives an overview of the employed model scenarios. In this study, we only focus on those 6 days when HCHO, CHOCHO, NMHCs, and OH measurements were available, i.e., 12–13, 20–21, and 24–25 July.

2.3 Model uncertainty

The uncertainty of the model simulation of HCHO and CHOCHO can arise from the uncertainty of (1) measured trace gas concentrations, (2) measured meteorological parameters, i.e., photolysis frequencies J, temperature T, and pressure P, (3) reaction rate constants k used in the model, and (4) the lifetime τ_D for dry deposition. Using the same uncertainty factors listed in Table S7 in Lu et al. (2012), we run the model base case (M0) for n times (n equals to the number of parameters been considered). During each model run, the value of the considered parameter is multiplied by its uncertainty factor. The model uncertainty is estimated by error propagation from the errors of all considered parameters. Gaussian error propagation was applied within each of the first three groups. The total model errors were then calculated conservatively by linear addition of the errors from all four groups. The mean diurnal variation of the uncertainty of the modeled HCHO and CHOCHO by the model base case is shown in Fig. S2. On average, modeled HCHO and CHOCHO concentrations in the model base case had an uncertainty of around 55 %.

3 Results

3.1 Measurements overview

The entire PRIDE-PRD campaign was characterized by tropical conditions with high temperature (28–36 °C), high

Table 1. Model scenarios used in the sensitivity study of HCHO and CHOCHO simulation during the PRIDE-PRD2006 campaign.

Simulation	Mechanisms	Purpose
M0	MCM v3.2 with $\tau_D = 24$ h	Base run
M1	as M0, but (1) change τ_D to 3 h for the time period of 06:00–19:00 in 13, 24, and 25 July, (2) decrease isoprene concentration to 52 % of the measured value for the period of 8:00–16:00, and (3) include measured PANs as model constraints	Influence of source terms
M2	as M1, but replace τ_D of HCHO and CHOCHO by $\tau_{\text{depo.}} = \frac{v_{\text{depo.}}}{\text{BLH}}$. $v_{\text{depo.}}$ is set to 1 cm s^{-1} and 0.3 cm s^{-1} for HCHO and CHOCHO, respectively.	Influence of dry deposition
M3	as M2, but add removal of all species by vertical dilution for the period of 06:00–10:00, with rate constant of 0.41 h^{-1}	Influence of vertical dilution
M4	as M3, but include uptake of HCHO and CHOCHO by aerosols, i.e., $\frac{dC}{dt} = -\frac{\gamma \times S_{\text{aw}} \times v \times C}{4}$ *, with an uptake coefficient γ of 10^{-3}	Influence of heterogeneous uptake

* C, v, and γ are the gas phase concentration, mean molecular velocity, and uptake coefficient, respectively. S_{aw} is the RH corrected aerosol surface concentration.

humidity (60–95 % RH), and high solar radiation (indicated by noontime J_{NO_2} of (5–10) $\times 10^{-3}$ s^{-1}) (Li et al., 2012). These meteorological conditions, together with the prevailing emissions of air pollutants, are in favor of the high photochemical reactivity in the PRD region, which can be reflected by the measured high OH concentrations (noontime value of 1.5×10^7 cm^{-3}) and HOx turnover rate (3×10^8 cm^{-3} s^{-1} around noon) (Hofzumahaus et al., 2009). For the 6 cloud-free days in this study, Fig. 1 shows the time series of measured wind speed, wind direction, OH reactivities of C2–C12 NMHC ($k_{\text{OH}}^{\text{NMHC}}$), OH concentrations, aerosol (PM_{10}) surface concentrations, aerosol (PM1) compositions, and HCHO and CHOCHO concentrations. The wind speeds were generally below 3 m s^{-1}. According to the wind direction, air masses arriving at the BG site were mainly from two directions, i.e., south on 20 and 21 July north on 13, 24, and 25 July. On 12 July, the wind was from north in the first night, and became south during daytime, and changed back to north after sunset. Peak values of $k_{\text{OH}}^{\text{NMHC}}$ were around 20 s^{-1} and normally occurred at night. Compared to southern wind days, elevated $k_{\text{OH}}^{\text{NMHC}}$ with average values of 5.6–6.7 s^{-1} were observed in the period of 09:00–18:00 in northern wind days, which was mainly attributed to the higher isoprene concentrations. This is consistent with the fact that north of BG site is close to forest areas and air masses from north are therefore influenced by biogenic emissions. However, average OH reactivities of anthropogenic NMHC for the same period were nearly the same in the 6 days, e.g., $k_{\text{OH}}^{\text{Alkene}} \approx 1.2$ s^{-1}, regardless of the origin of air masses. OH concentrations also do not show big difference in the 6 days, with peak values of 1.5×10^7 cm^{-3} around noon and values of 0–1 $\times 10^6$ cm^{-3} during night. The aerosol (PM1) composition measurements found that almost half of the sub-micron aerosol mass consisted of organics, and the the next most found substance was sulfate. On 24 and 25 July when strong combustion events happened in the surrounding areas, the aerosol mass and surface concentrations were significantly higher than in other days. The occurrence of the combustion events can be indicated by the increase of Cl^- concentration in PM1 (Hu et al., 2012). This Cl^- increase is identified in the early morning of 13, 24, and 25 July and around mid-night of 25 July. Increase of $k_{\text{OH}}^{\text{Alkene}}$ was also observed in the combustion periods. In the 6 cloud-free days, the measured average concentrations of HCHO and CHOCHO were 7.3 ppb and 0.37 ppb, respectively. Elevated HCHO and CHOCHO concentrations were observed during periods when combustion events were prevailing. Diurnal variability of HCHO and CHOCHO was not very prominent. After excluding the periods influenced by combustion events, a slight increase of HCHO concentrations can be found from early morning to 12:00, whereas CHOCHO concentrations are almost stable at around 0.3 ppb.

3.2 HCHO and CHOCHO simulation by the model base case

The simulated HCHO and CHOCHO concentrations from the model base case (M0) are shown in Fig. 2. Neither the observed diurnal variation nor the concentration can be well reproduced by the model. The model predicts HCHO maxima occurring at around 09:00 with concentrations of 30–40 ppb, followed by decrease of HCHO concentration to 10–25 ppb from late morning to afternoon. In the afternoon, the simulated HCHO are separated into two groups; higher calculated concentrations are found when the wind is coming from the north of the BG site. This phenomenon also exists for the modeled CHOCHO. In general, the model base case overpredicts HCHO and CHOCHO concentrations by factors of 2–6. While the measurements did not find prominent diurnal variation of CHOCHO/HCHO ratios (R_{GF}), the model shows

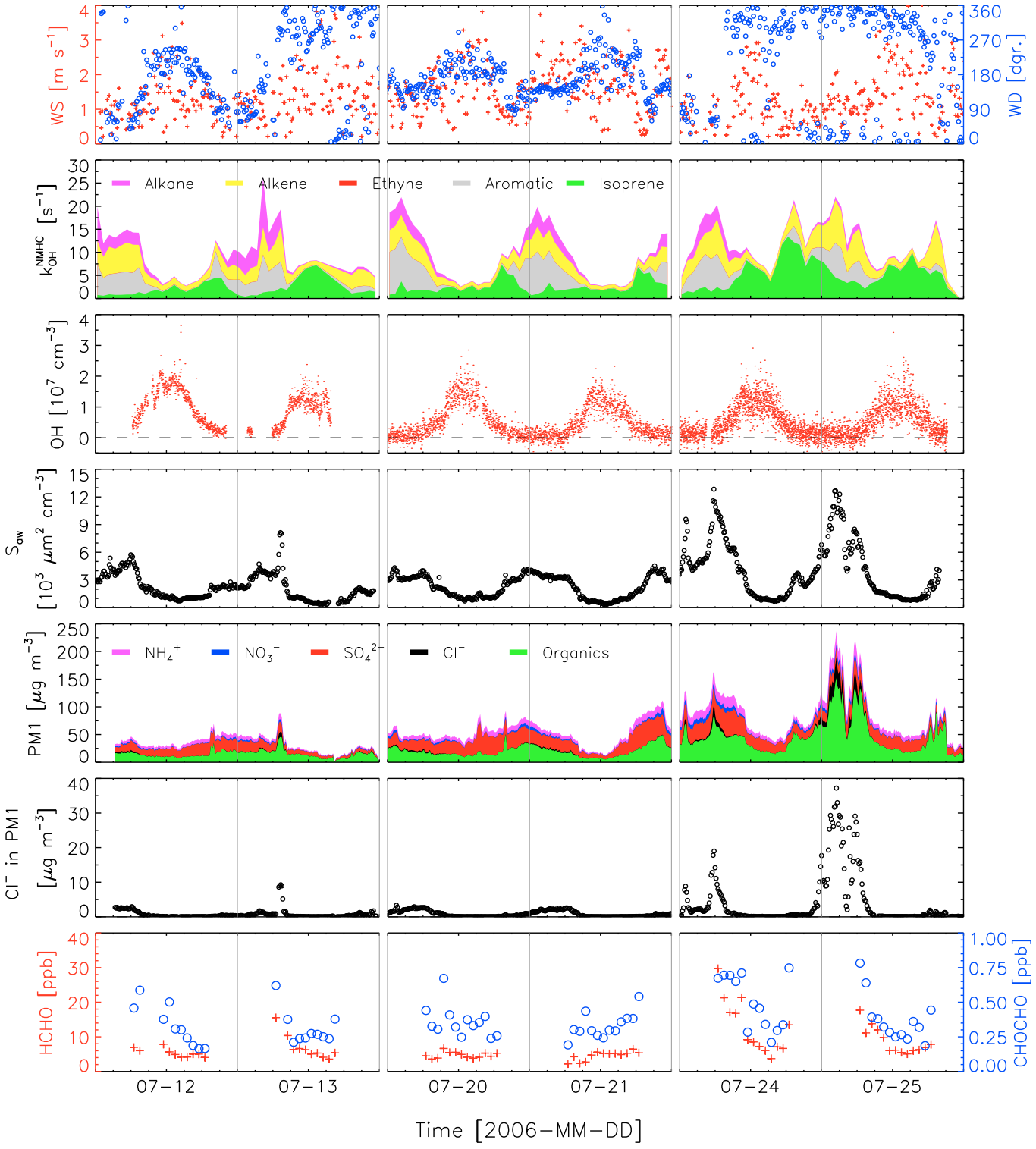

Figure 1. Time series of wind speed (WS), wind direction (WD), OH reactivity of measured C3–C12 NMHCs (k_{OH}^{NMHC}), OH, aerosol (PM_{10}) surface concentration (S_{aw}, i.e., S_a corrected for hygroscopic growth), aerosol (PM1) compositions, HCHO, and CHOCHO for the 6 cloud-free days during the PRIDE-PRD2006 campaign. S_{aw} is the RH corrected aerosol surface concentration, i.e., $S_{aw} = S_a \times f(RH) = S_a \times (1 + a \times (RH)^b)$. The empirical factors a and b used to estimate $f(RH)$ were set to 2.06 and 3.6 as described by Liu et al. (2008).

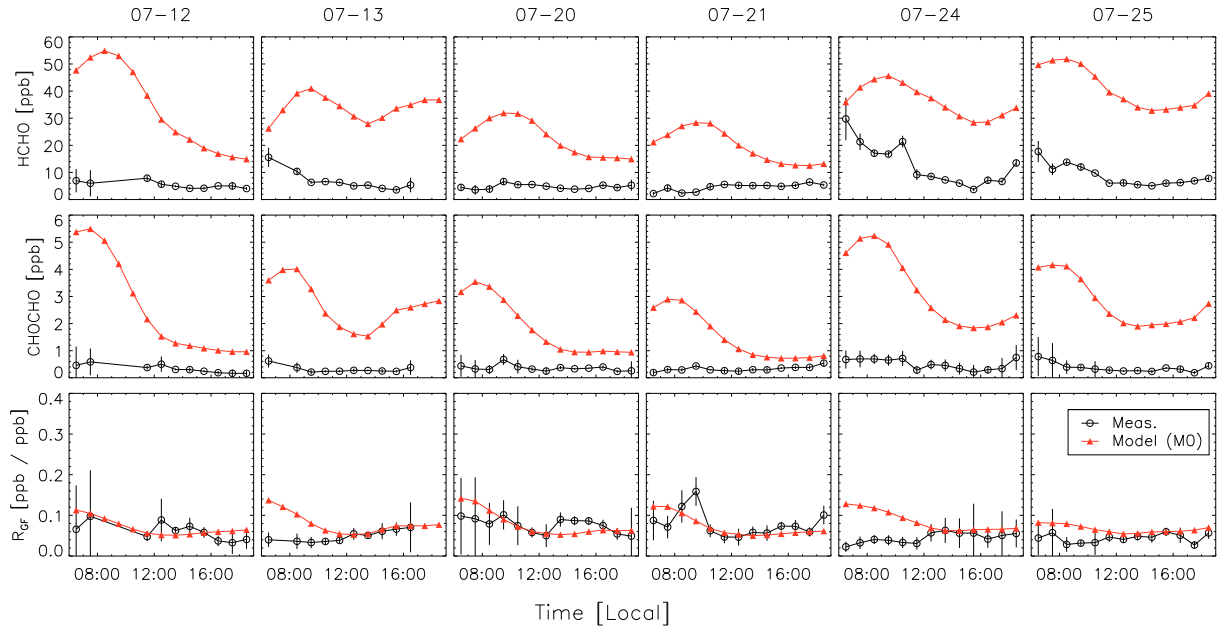

Figure 2. Measured and modeled HCHO, CHOCHO, and CHOCHO/HCHO ratios (R_{GF}) for the 6 cloud-free days during the PRIDE-PRD2006 campaign. The modeled values are from the model base case (M0). The error bar refers to the 1σ statistic error of the measurements.

a decrease of R_{GF} from morning to noon and stable R_{GF} values in the afternoon (Fig. 2). Compared to the discrepancy for the HCHO and CHOCHO concentrations, the R_{GF} calculated by the model (0.075 ± 0.024) is only slightly higher than that by the measurements (0.059 ± 0.024).

The contribution of different measured NMHCs to the production of HCHO and CHOCHO in the model base case is shown in Fig. 3. On average, isoprene oxidation contributes most to the HCHO production (43 %), followed by the oxidation of alkenes (29 %), aromatics (15 %), and alkanes (13 %). For CHOCHO, half of its production is due to isoprene oxidation, and the other half is dominated by aromatics oxidation. The contributions of alkanes, alkenes, and ethyne to the total CHOCHO production are in total less than 10 %. The top-10 precursor NMHCs of HCHO and CHOCHO in terms of their production rate are listed in Table 2. Compared to similar studies (e.g., Volkamer et al., 2010; Huisman et al., 2011; Washenfelder et al., 2011; MacDonald et al., 2012; Parrish et al., 2012), anthropogenic and biogenic sources contribute almost equally to the chemical formation of HCHO and CHOCHO at the BG site. However, production of HCHO and CHOCHO from anthropogenic precursors is larger than from isoprene before noon; in the afternoon, the contribution of isoprene to HCHO and CHOCHO production becomes higher than from anthropogenic NMHCs. This diurnal variation is the result of the change of air mass composition, i.e., from anthropogenically to biogenically dominated. The transition of air mass composition during daytime at the BG site has also been illustrated by Lu et al. (2012) during the analysis of the HOx budget.

Maximum production of HCHO and CHOCHO in the model always occurs at around noon, coinciding with the peak of OH concentrations. We investigated the production of HCHO and CHOCHO from the oxidation of NMHCs by different oxidants (i.e., OH, O_3, and NO_3). In general, OH initiated oxidation of NMHCs accounts for most of the local production rate of HCHO and CHOCHO (> 95 %) throughout the day; ozonolysis and oxidation by NO_3 are of minor importance. Compared to HCHO, we did not find any contribution of ozonolysis of alkenes to the CHOCHO formation. With regard to the oxidation of NMHCs by NO_3, its contribution to the CHOCHO production is larger than to the HCHO production. The nighttime production of HCHO and CHOCHO from OH initiated oxidation of NMHCs results in the maximum concentration of HCHO and CHOCHO occurring in early morning hours. Without existence of OH during night, the lifetime of HCHO and CHOCHO in the model is determined by dry deposition (i.e., τ_D = 24 h), and the production of HCHO and CHOCHO from O_3 and NO_3 reactions is quite small. Therefore, modeled HCHO and CHOCHO concentrations during night are determined mainly by the concentrations the day before. In a model run with nighttime OH concentration fixed to zero, compared to the model base case results, HCHO and CHOCHO show much lower concentrations during night and reach their peak concentration at a later time (≈2 h) (Fig. S3).

In the model base case, the destruction of HCHO and CHOCHO can be expressed as the sum of first order reaction rates of reaction with OH, photolysis, and dry deposition, i.e., k_d^{HCHO} and k_d^{CHOCHO}. It is found that reaction with

Table 2. Top-10 precursor NMHCs of HCHO and CHOCHO for the 6 cloud-free days during the PRIDE-PRD2006 campaign.

NMHCs	P_{HCHO} ppb h^{-1}	%	NMHCs	P_{CHOCHO} ppb h^{-1}	%
Isoprene	3.85	43.2	Isoprene	0.37	51.5
Propene	0.97	12.8	Toluene	0.17	22.0
Ethene	0.67	8.2	Ethylbenzene	0.04	5.2
Stryrene	0.24	6.1	m-Xylene	0.04	5.1
Methane	0.30	4.2	Ethene	0.03	4.2
m-Xylene	0.33	3.2	Benzene	0.03	4.0
1-Butene	0.17	2.5	o-Xylene	0.02	2.8
trans-2-Butene	0.18	2.2	Ethyne	0.02	2.4
Toluene	0.21	1.9	1,2,4-Trimethylbenzene	0.01	1.3
cis-2-Butene	0.15	1.7	o-Ehtylbenzene	0.004	0.5

Table 3. Relative changes of HCHO and CHOCHO mixing ratio and R_{GF} under different model simulations (Table 1) for the PRIDE-PRD2006 campaign. When the model scenario is changing from M_i to M_j $(i, j \in [0, 4])$, the relative change in percentage is calculated as $\% = 100 \times (M_j - M_i)/M_i$.

Model	Time period	Relative change in %		
		HCHO	CHOCHO	R_{GF}
M0 → M1	06:00–18:00	−49	−37	22
	06:00–10:00	−41	−22	31
	10:00–18:00	−53	−44	18
M1 → M2	06:00–18:00	−16	−7	13
	06:00–10:00	−34	−16	30
	10:00–18:00	−7	−3	4
M2 → M3	06:00–18:00	−25	−30	−8
	06:00–10:00	−36	−40	−7
	10:00–18:00	−19	−26	−9
M3 → M4	06:00–18:00	−49	−45	4
	06:00–10:00	−66	−71	−14
	10:00–18:00	−40	−32	13
M0 → M4	06:00–18:00	−84	−79	30
	06:00–10:00	−92	−89	38
	10:00–18:00	−80	−74	26

OH and photolysis are responsible for 90 % of the HCHO and CHOCHO removal during daytime. During night, HCHO and CHOCHO are removed mainly by dry deposition (60 %); the observation of nighttime OH with concentrations of around 10^6 cm^{-3} accounts for the rest. The lifetime of HCHO (reciprocal of k_d^{HCHO}) is more than 10 h during night and decreases to around 1.3 h at noon. CHOCHO has a similar lifetime as HCHO during the campaign.

4 Discussion

4.1 Reconciliation between the modeled and the measured HCHO and CHOCHO

Compared to the model base case results, our measurements at the BG site show much lower concentrations of HCHO and CHOCHO which can not be explained by the uncertainties of model and measurements. Moreover, observed concentrations in the afternoon hours do not separate into different groups. To identify the explanation for these discrepancies, we performed a number of sensitivity model runs (Tables 1 and S2). Given that direct emissions of HCHO and CHOCHO are not considered in the model, periods which are under the influence of local emissions (i.e., early morning of 13, 24, and 25 July) are excluded from the analysis in this section.

The simulated HCHO and CHOCHO concentrations in the model are determined by their production and destruction processes. The employed box model could inherently overestimate the yield of HCHO and CHOCHO in the oxidation of different NMHCs. In the model base case, isoprene, alkenes and aromatics are the major precursors of HCHO and CHOCHO (Fig. 3). Firstly, when strong emission sources of these NMHCs exist in the nearby area, the model might not be in steady state resulting in an overestimation of secondary products. Secondly, HCHO and CHOCHO concentrations derived from MAX-DOAS measurements represent the average value over a certain horizontal and vertical space. During the 6 cloud-free days, as estimated from the MAX-DOAS measured boundary layer height (BLH) and the visibility inside the boundary layer, the horizontal and vertical extension of the observation volume were both within ≈2 km (Li et al., 2010). If the air mass in this volume was not well mixed, different HCHO and CHOCHO production rates compared to the rates calculated from the locally measured OH, NMHCs, etc. would be the consequence. Since HCHO and CHOCHO are mainly coming from the reaction of OH with NMHCs, the above effects can be tested through the sensitivity of the

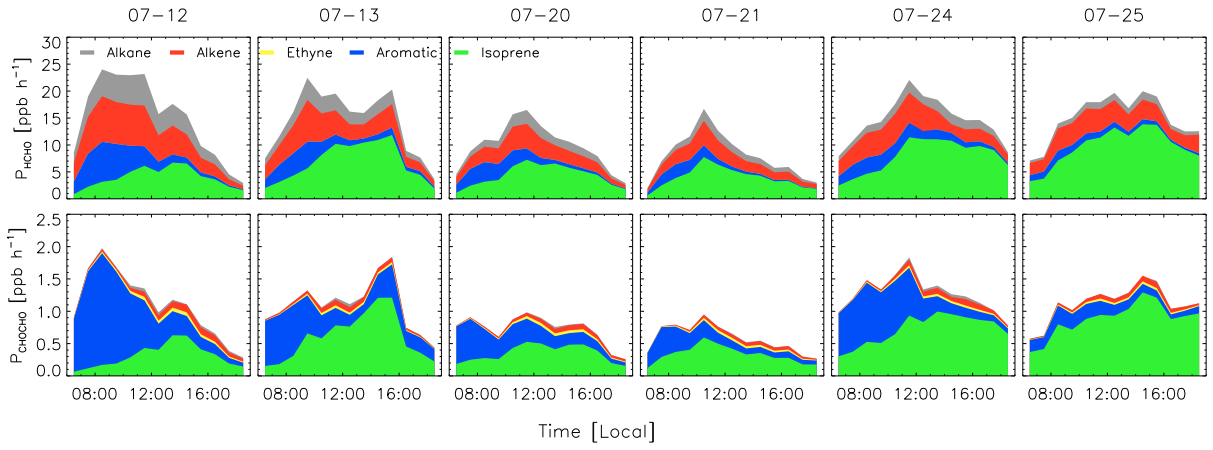

Figure 3. Production of HCHO and CHOCHO from different NMHCs precursors in the model base case (M0) for the 6 cloud-free days during the PRIDE-PRD2006 campaign.

modeled HCHO and CHOCHO on both (1) different τ_D values and (2) different OH and NMHC concentrations.

The parameter τ_D can be used as a scale of the generic removal of species included in the model. The shorter the τ_D, the faster the removal, resulting in less reaction time Δt (i.e., similar to the photochemical age as used by Fried et al. (2011)) and less oxidation products of primary emitted NMHCs. As described by Lou et al. (2010), oxidation product of the measured NMHCs account for more than 50 % of the measured total OH reactivity (k_{OH}) at the BG site. Therefore, once τ_D deviates from the real value, modeled k_{OH} will become different than measured k_{OH}. While τ_D = 24 h, good agreement between modeled and measured k_{OH} is found in most periods during the campaign. However, on 13, 24, and 25 July when strong isoprene emission existed at the north of the BG site, the value of τ_D during daytime needs to be reduced to 3 h to let the modeled k_{OH} match the measured k_{OH} (Fig. S4), indicating the shorter photochemical age of the measured air mass in these than in the other time periods. It is most likely that the air mass with freshly emitted isoprene was not photochemically degraded when it was detected. Decrease of τ_D from 24 h to 3 h results in an average decrease of modeled daytime (06:00–18:00) HCHO and CHOCHO concentrations by 31 % of the values in the model base case (Fig. S4).

Decrease of OH concentration by 20 % can result in a maximum decrease of modeled HCHO and CHOCHO concentration by 16 % and 20 %, respectively. The reconciliation between modeled and measured HCHO (CHOCHO) concentration would require OH concentration to be decreased to < 30 % of the measured value (Fig. S3). Similar sensitivity results are found for the NMHC concentrations (Fig. S5). Within $\approx$2 km along the MAX-DOAS viewing direction, the land is covered homogeneously by trees. It is unlikely that OH or NMHC concentrations differ by a factor of 2–3 from the local measurements. However, it is possible that some short-lived NMHCs have strong vertical gradients due to vertical mixing. At around noon, the typical mixing time for a species in a well developed convective boundary layer is about 15 min (c.f. Stull, 1988). Given the observed noontime OH concentration of 1.5×10^7 cm^{-3}, this mixing time is longer than the lifetime of isoprene ($\approx$ 10 min) but is much shorter than the lifetime of aromatics and other alkenes at the BG site. Therefore, it has to be expected that isoprene emitted at ground level would not be well-mixed in the boundary layer within its lifetime. Assuming a vertical exponential decay of the isoprene concentration in the boundary layer and using the measured noontime BLH of around 2 km, the effective average isoprene concentration in the boundary layer is estimated to be only 52 % of the measured value at ground (i.e., the value used in the model base case). For the time period when convective mixing is strong, i.e., 08:00–16:00, we reduced the isoprene concentration in the model to 52 % of the measured value. Compared to the model base case, this change results in an average decrease of modeled HCHO and CHOCHO concentration by 15 % for this time period (Fig. S5). The decrease is larger (up to 35 %) for days when the BG site was influenced by strong isoprene emissions (i.e., 13, 24, and 25 July).

Together with the formation of HCHO and CHOCHO, hydroperoxides (e.g., H_2O_2, CH_3OOH), and peroxyacyl nitrates (PANs) are produced in the oxidation of NMHCs. So, using these measurement results as additional constraints in the model, the prediction of NMHC oxidation processes can be improved (Kormann et al., 2003). It is found that the model run with measured H_2O_2 and CH_3OOH gives nearly the same HCHO and CHOCHO concentrations as in the model base case (Fig. S6). Including measured PANs in the model can only lead to a maximum reduction of modeled HCHO concentration by 30 % (Fig. S7). Modeled HCHO and CHOCHO seem not to be sensitive to the change of hydroperoxide and PAN abundances.

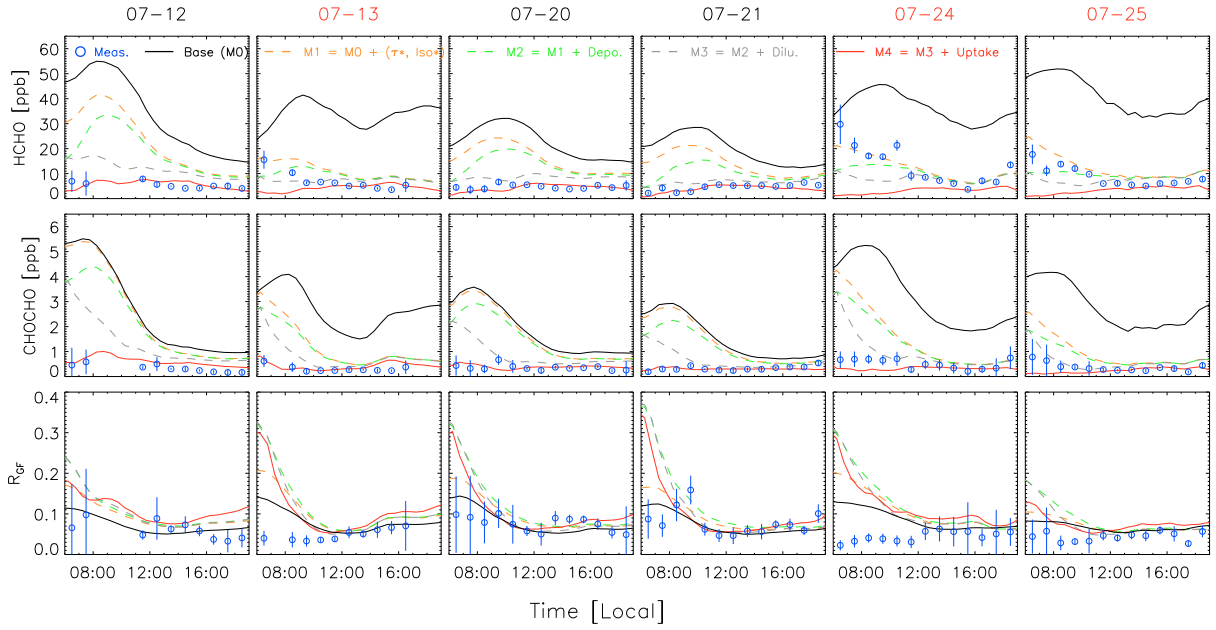

Figure 4. Sensitivity analysis of HCHO and CHOCHO simulation for the 6 cloud-free days during the PRIDE-PRD2006 campaign. Dates color coded in red are the days which were influenced by local combustion events. The blue dots are the measured concentrations with error bars indicating the 1σ statistic error of the measurements. Symbols with color black, orange, green, gray, and red represent the modeled concentrations by model base case (M0), and M1–M4, respectively. Detailed model settings are described in Table 1 in the text.

By using modified τ_D values and isoprene concentrations in the model, and by including PAN measurements as additional model constraints (model scenario M1), the modeled HCHO (CHOCHO) concentrations during daytime (06:00–18:00) decrease by 67 % (60 %) of the values in the model base case for 13, 24, and 25 July and by 31 % (13 %) for 12, 20, and 21 July. Given the uncertainties of model and measurements, the model results agree with the measurements of 13, 24, and 25 July but are still twice as high as the measured values for 12, 20, and 21 July (Fig. 4). Therefore, the uncertainties of the production terms of HCHO and CHOCHO in the model can only partly explain the discrepancy between modeled and measured concentrations. As a consequence, HCHO and CHOCHO sink terms are most likely underestimated by the model.

Missing HCHO and CHOCHO sinks can originate either from the range of the existing HCHO and CHOCHO destruction terms in the model (i.e., reaction with OH, photolysis, and dry deposition), or from horizontal advection, vertical dilution, or loss on aerosol surfaces which are not considered in the model.

We showed above that the sensitivity of modeled HCHO and CHOCHO on the change of OH concentration can not explain the overestimation of HCHO and CHOCHO concentration. Since all days mentioned in this paper showed clear-sky conditions, the photolysis frequency measurements were representative enough for the entire MAX-DOAS observation volume. Given that the photolysis frequency measurements have an accuracy of 10 %, they can only have a minor influence on the overestimation.

Dry deposition of trace gases was included in the model by a constant lifetime $\tau_D = 24$ h, which corresponds to a deposition velocity of 1.6 cm s^{-1} when taking the average measured daytime BLH of 1.4 km. The reported deposition velocities of HCHO and CHOCHO are 0.05–1 cm s^{-1} (Stickler et al., 2006) and 0.15–0.3 cm s^{-1} (c.f., Washenfelder et al., 2011), respectively. Though the average loss of HCHO and CHOCHO through dry deposition in the model base case is faster than reported, it does not take the diurnal variation of boundary layer into account. During night, assuming a BLH of 100 m, a deposition velocity of 1 cm s^{-1} results in a lifetime of 2.8 h which is an order of magnitude shorter than the τ_D of 24 h. This means the loss of HCHO and CHOCHO during night should be faster than the model base case predicted. Based on the model scenario M1, we replaced the constant τ_D of HCHO (CHOCHO) by a time dependent lifetime calculated from the measured BLH (assume nighttime value of 100 m) and a deposition velocity of 1 cm s^{-1} (0.3 cm s^{-1}) (model scenario M2). As shown in Fig. 4, for morning hours (06:00–10:00), the calculated HCHO and CHOCHO concentrations by the model scenario M2 decrease by 34 % and 16 % of the values by the model scenario M1, respectively. However, the influence of dry deposition on the modeled HCHO and CHOCHO is marginal during the afternoon.

If the air mass detected by MAX-DOAS was inhomogeneously mixed, the HCHO and CHOCHO concentrations

calculated from locally measured OH, NMHCs, etc. could be different from that at other points. This will result in HCHO and CHOCHO concentration gradients, and lead to HCHO and CHOCHO transport through horizontal advection. During daytime, considering the short lifetime of HCHO and CHOCHO (≈1.5 h), the low wind speed (≈ 2 m s^{-1}) at the BG site, and the homogeneous type of land usage along the MAX-DOAS viewing direction, horizontal advection might have only a minor influence on the HCHO and CHOCHO simulation.

With regard to the vertical dilution which is caused by the mixing of the shallow (but growing) mixing layer with the nocturnal boundary layer and with the residual layer between sunrise and noon, we can estimate the dilution rate to be constant (k_{dilu}) from the decay of the measured black carbon concentrations. During the campaign, the black carbon concentration usually experienced a fast decrease around sunrise (i.e., 06:00–10:00) and showed stable values after 11:00 until sunset. The diurnal variation of the black carbon concentration indicates an efficient vertical dilution in the period of 06:00–10:00, and a well mixed boundary layer since 11:00. In the 6 modeling days, the calculated k_{dilu} ranges from 0.2 to 0.61 h^{-1} with an average value of 0.41 h^{-1}. Assuming a constant k_{dilu} of 0.41 h^{-1}, we applied this removal to all species by vertical dilution for the time period of 06:00–10:00 in the model scenario M2 (i.e., model scenario M3). Compared to the model scenario M2, significant decrease (by ≈ 40 %) of modeled HCHO and CHOCHO concentrations can be identified during morning hours (Fig. 4).

In addition to the modification of production terms of HCHO and CHOCHO in the model, including vertical dilution and modified dry deposition (model scenario M3) results in reasonable agreement between modeled and measured HCHO and CHOCHO concentrations in most of the time during the 6 cloud-free days (Fig. 4). However, during early morning hours (06:00–09:00), the modeled CHOCHO concentrations are still significantly higher than the measured values. For days without the influence of direct precursor emission in the morning (i.e., 12, 20, and 21 July), the modeled HCHO concentrations are also higher than the measured values.

Laboratory and field studies indicate that HCHO and CHOCHO in the gas phase can be lost on aerosols through heterogeneous uptake processes (Volkamer et al., 2007; Wang et al., 2010; Li et al., 2011; Washenfelder et al., 2011; Toda et al., 2014). This uptake process has been shown to be related to the acidity (Jayne et al., 1996; Liggio et al., 2005) or the ionic strength (Kroll et al., 2005) of aerosols. Using an online Aerosol Inorganics Model (AIM, Model II) (http://www.aim.env.uea.ac.uk/aim/model2/model2a.php) and the method described by Zhang et al. (2007), we estimated H^+ activity a_{H^+} and ionic strength within the aqueous particle phase from aerosol mass spectrometry (AMS) measurements of NH_4^+, SO_4^{2-}, NO_3^-, and Cl^- in PM1. During the daytime of the 6 cloud-free days, the average value of the calculated a_{H^+} was 1.47×10^{-2} mol L^{-1} (corresponding to a pH value of 1.8), indicating high aerosol acidity at the BG site. Given the high aerosol concentrations in the early morning hours (Fig. 1), we investigated the sensitivity of modeled HCHO and CHOCHO concentrations on heterogeneous uptake processes (i.e., model scenario M4). Using an uptake coefficient of 10^{-3} as indicated by laboratory and field studies (Jayne et al., 1996; Liggio et al., 2005; Volkamer et al., 2007), the calculated CHOCHO concentration by the model scenario M4 decrease significantly (by ≈ 70 %) from that by the model scenario M3 for the early morning hours. In the afternoon, due to decreased aerosol concentration, the influence of the uptake by aerosols on the modeled CHOCHO concentrations becomes small. Compared to the model scenario M3, the model scenario M4 provides better agreement between modeled and measured HCHO and CHOCHO concentrations (Fig. 4). Under tropospheric conditions, while the uptake coefficient of 10^{-3} can be realistic for CHOCHO, there remains a large uncertainty for HCHO. The value of 10^{-3} used in the model scenario M4 for HCHO is estimated from laboratory studies representing typical conditions in the upper troposphere or in the stratosphere (i.e., low temperature and high aerosol acidity) (Jayne et al., 1996). During experiments performed under tropospheric conditions by Kroll et al. (2005), no uptake of HCHO by aerosols was observed. However, some laboratory (Sassine et al., 2010; Li et al., 2011) and field (Wang et al., 2010; Toda et al., 2014) studies identified loss of HCHO on tropospheric aerosols under certain conditions. Therefore, it is possible that the use of 10^{-3} as the HCHO uptake coefficient could not well represent the condition at the BG site.

Table 3 summarized the relative changes of modeled HCHO and CHOCHO concentrations by adding additional processes to the model base case (i.e., model scenarios M1–M4). By including additional production and destruction terms (i.e., model scenario M4), the modeled HCHO and CHOCHO concentrations during daytime (06:00–18:00) decrease by ≈ 80 % of the values predicted by the model base case. On average, the production terms (i.e., deviation from steady-state, vertical transport of isoprene) and the uptake by aerosols have the largest effect (≈ 50 %) on the concentration decrease, followed by vertical dilution (≈ 30 %) and deposition (≈ 15 %). Increased influence of vertical dilution and deposition on the concentration decrease can be found for morning hours.

4.2 Influences on the CHOCHO to HCHO ratio

As illustrated by Vrekoussis et al. (2010) and DiGangi et al. (2012), the CHOCHO to HCHO ratio (R_{GF}) can be used as an indicator of anthropogenic or biogenic impact on photochemistry. When HCHO and CHOCHO are entirely photochemically formed, R_{GF} is determined by the relative strength of production and destruction of HCHO and CHOCHO. When the system is in steady-state, R_{GF} can be

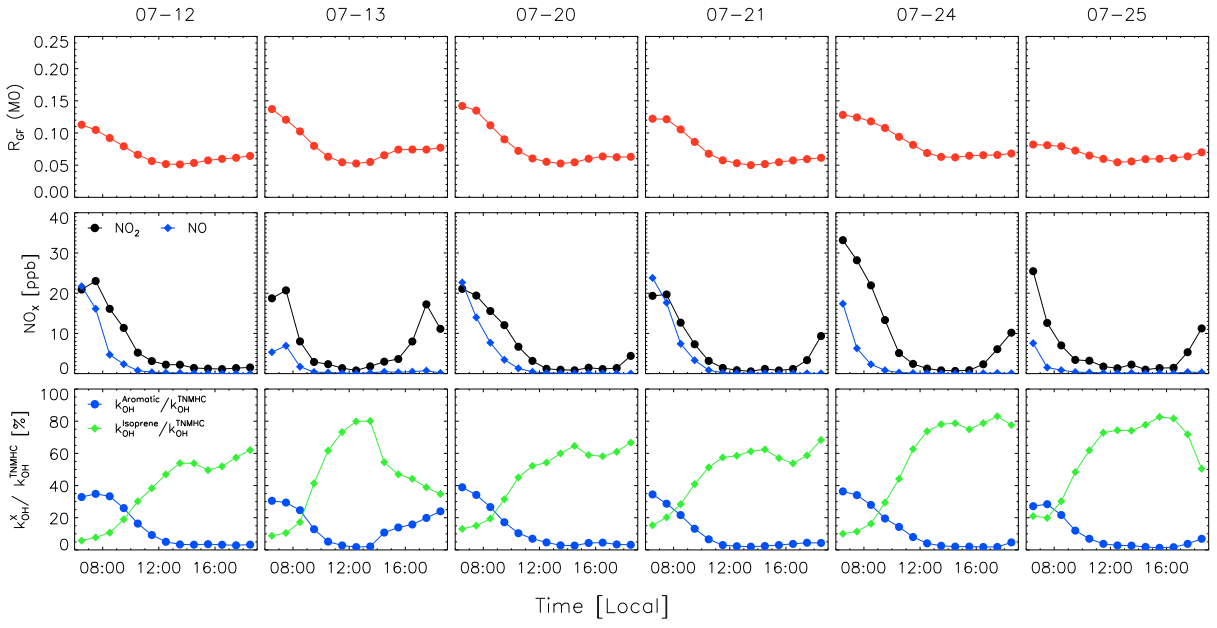

Figure 5. Time series of modeled R_{GF} (by the model base case), measured NO and NO_2 concentrations and NMHC compositions for the 6 cloud-free days during the PRIDE-PRD2006 campaign. The NMHC composition is expressed as the fraction of OH reactivity of a certain type of NMHC to that of the total NMHC.

expressed as

$$R_{GF} = \frac{[CHOCHO]}{[HCHO]} = \frac{P_{CHOCHO}}{P_{HCHO}} \cdot \frac{k_d^{HCHO}}{k_d^{CHOCHO}}. \quad (1)$$

Given a certain OH concentration, photolysis frequencies, and deposition rate, k_d^{HCHO}/k_d^{CHOCHO} is well defined, and R_{GF} depends on P_{CHOCHO}/P_{HCHO}. P_{CHOCHO}/P_{HCHO} is largely influenced by the NMHC composition of the investigated air mass.

In the 6 cloud-free days during the PRIDE-PRD2006 campaign, the average value of measured and modeled (by the model base case) R_{GF} is 0.059 ± 0.024 and 0.075 ± 0.035, respectively. In addition to photochemical processes, direct emissions also contribute to ambient HCHO concentrations (Garcia et al., 2006), which would lead to a decease of R_{GF}. Due to the lack of information on the primary HCHO sources for areas around the BG site, HCHO emission were not included in our model. However, in the early morning of 13, 24, and 25 July when combustion events were prevailing in the surrounding areas of the BG site, we found high HCHO concentrations and low R_{GF} (≈ 0.03). So, there is a possibility that some HCHO primary sources existed in the surrounding area, which causes the discrepancy between modeled and measured R_{GF}.

On the other hand, the model base case can be used to investigate the influence of different chemical processes on the variation of R_{GF}. Given the similarity of the photochemical processes of HCHO and CHOCHO, R_{GF} shows little sensitivity on the total NMHC reactivities (k_{OH}^{TNMHC}). When k_{OH}^{TNMHC} in the model are decreased to half of the measured values, P_{CHOCHO} and P_{HCHO} are decreased similarly by 46 % on average. As a result, R_{GF} remains the same as before. However, R_{GF} slightly depends on the OH level. With the decrease of OH concentration, both P_{CHOCHO}, P_{HCHO}, k_d^{HCHO}, and k_d^{CHOCHO} are found to be decreasing but to different extents. When OH concentration is decreased to 50 % of the measured values, the decrease of k_d^{HCHO} and k_d^{CHOCHO} are similar (i.e., by 28 % on average), but the decrease of P_{CHOCHO} (by 55 % on average) is stronger than that of P_{HCHO} (by 49 % on average). This results in an average decrease of R_{GF} by 12 %. The different dependence between P_{HCHO} and P_{CHOCHO} on OH concentration is caused by the fact that HCHO and CHOCHO are produced at different generations of NMHCs oxidation by OH. At the BG site, oxidation of isoprene and alkenes by OH is the major process producing HCHO (Sect. 3.2). During this process, HCHO is mostly produced as a first generation product and only one OH radical is consumed when each HCHO is generated. Therefore, P_{HCHO} is almost linearly dependent on OH concentration. However, this situation is different for CHOCHO. Under the conditions at the BG site, we found that CHOCHO is mostly the third or forth generation product of isoprene and aromatic oxidation by OH. Generating one CHOCHO molecule needs more than one OH radical, which leads to a non-linear dependence of P_{CHOCHO} on OH.

Looking at the time series of modeled R_{GF} (Fig. 5), high R_{GF} is usually found in early morning and a sharp decrease of R_{GF} is identified shortly after sunrise. This

pattern follows the diurnal variation of NO_x concentrations and of the contribution of aromatics to the total NMHC reactivities ($k_{OH}^{Aromatics}/k_{OH}^{TNMHC}$), but is opposite to that of the contribution of isoprene to the total NMHC reactivities ($k_{OH}^{Isoprene}/k_{OH}^{TNMHC}$), thereby indicating a positive (negative) impact of the anthropogenic (biogenic) emissions on R_{GF}. A similar phenomenon was observed by DiGangi et al. (2012) at a rural site in the USA. Our model shows that P_{CHOCHO}/P_{HCHO} of aromatic compounds (e.g., benzene, toluene, m,p-xylene) are more than 3 times larger than that of isoprene. The P_{CHOCHO}/P_{HCHO} of alkanes and alkenes are even smaller than that of isoprene, due to the little contribution of alkanes and alkenes to the CHOCHO production. Therefore, higher R_{GF} can be expected when NMHC concentration is dominated by aromatics. Besides the NMHC composition, NO_x levels can also influence the R_{GF} since HCHO and CHOCHO have different sensitivities to the change of NO_x concentrations. The NO level determines the conversion of RO_2 to RO which finally produces HCHO and CHOCHO. When the NO concentration in the model is increased, a larger concentration increase is found for HCHO than for CHOCHO leading to a decrease of R_{GF}. This is because the contribution of RO decomposition to the HCHO formation is larger than to the CHOCHO formation at the BG site. At low-NO, $RO_2 + HO_2$ reaction forming hydroperoxides competes with $RO_2 + NO$. Therefore, the sensitivity of R_{GF} to NO is found to be low and high in high- and low-NO regimes, respectively. In general, an increase of NO concentration by 1 % results in a decrease of R_{GF} by 0–0.2 %. In contrast to NO, an increases of NO_2 causes an increase of R_{GF}. This is because, compared to HCHO, the modeled CHOCHO is more sensitive to NO_2. Change of NO_2 concentrations can have an influence on OH (via $OH + NO_2$) and NO_3 concentrations. Since the OH concentration in the model is constrained to the measurements, CHOCHO and HCHO formation through OH initiated NMHC degradations will only be marginally affected when the NO_2 concentration is increased / decreased. Since the NO_3 reactions have different contribution to the HCHO and CHOCHO production (Sect. 3.2), increase of the modeled NO_3 concentration as a result of the increase of NO_2 can cause the change of R_{GF}. It is found that the change of R_{GF} ranges from 0 to 0.3 % when the NO_2 concentration is changed by 1 %; the lower the NO_2 concentration, the higher the sensitivity of R_{GF} to NO_2.

Based on above analysis, the modeled diurnal variation of R_{GF} can be explained by the existence of nighttime OH, by the change of NMHC composition, and by the NO_x concentration. During night, the existence of significant amounts of OH radicals made the OH + NMHC reactions the major pathway of HCHO and CHOCHO formation. The increase of R_{GF} after sunset is then the result of the increase of $k_{OH}^{Aromatics}/k_{OH}^{TNMHC}$ and of the NO_2 concentration; and the slowing down of the R_{GF} increase is caused by the occurrence of high NO concentrations later on. Around sunrise, due to the decrease of $k_{OH}^{Aromatics}/k_{OH}^{TNMHC}$ and of the NO_x concentration, and the earlier occurrence of CHOCHO photolysis (compared to HCHO, the absorption cross section of CHOCHO extends more to the visible wavelength range), the decrease of P_{CHOCHO}/P_{HCHO} and of k_d^{HCHO}/k_d^{CHOCHO} lead to the decrease of R_{GF} in the model. When setting the nighttime OH concentration to zero, modeled HCHO and CHOCHO concentrations during night are then mainly determined by their production in the previous afternoon which are mostly determined through isoprene oxidation (Sect. 3.2). As a result, modeled R_{GF} during night are as low as those during the previous afternoon when total NMHC reactivity was dominated by isoprene.

In addition to the above factors, additional processes included in the model scenarios M1–M4 also influence the CHOCHO to HCHO ratio (R_{GF}). As shown in Table 3 and Fig. 4, from noon to the afternoon, the modeled R_{GF} in the model scenario M4 increase by 30 % of the values in the model base case. Larger increase of R_{GF} can be found during early morning hours, mainly caused by the faster removal of HCHO by dry deposition than that of CHOCHO. Different from other processes, vertical dilution generally causes a small decrease of R_{GF}.

By analyzing satellite measurement results, Vrekoussis et al. (2010) concluded that high R_{GF} can represent regions strongly influenced by biogenic emissions. However, based on the in situ observations, DiGangi et al. (2012) found that the anthropogenic emissions have positive impact on R_{GF}. Our model study at the BG site indicate that the influence of anthropogenic emissions on R_{GF} is rather complicated. On the one hand, anthropogenic emissions of aromatics and NO_2 can contribute to the increase of R_{GF}. On the other, both emitted NO and HCHO can lead to a decrease of R_{GF}. For example, compared to the period of 12:00–18:00 on 21 July although the contribution of aromatics to k_{OH}^{TNMHC} is lower than on 24 July the lower NO and higher NO_2 concentrations during 24 July caused higher modeled R_{GF}. Moreover, processes like dry deposition and uptake by aerosols also have influence on R_{GF}.

5 Summary and conclusion

HCHO and CHOCHO are trace gases produced through the oxidation of NMHCs. High vertical column densities of HCHO and CHOCHO have been observed by satellite measurements for the Pearl River Delta (PRD) region in southern China, indicating the existence of high photochemical reactivity. However, investigations on the sources and sinks of HCHO and CHOCHO in the PRD are rather limited. During the PRIDE-PRD2006 campaign, MAX-DOAS observations of HCHO and CHOCHO together with measurements of HO_X radicals, trace gases, aerosols, and meteorological parameters were performed at the semi-rural site, Back Garden (BG), in the PRD. Using these measurement results and

a box model, we investigated production and destruction processes of HCHO and CHOCHO for 6 cloud-free days during the campaign.

The production of HCHO and CHOCHO at the BG site took place under the combined influence of anthropogenic and biogenic emissions. OH initiated oxidation of isoprene accounts for nearly half of the HCHO and CHOCHO formation, with increased contribution in the afternoon. The anthropogenic source of HCHO includes the degradation of alkenes (29 %), aromatics (15 %), and alkanes (13 %). Besides isoprene, most of the CHOCHO production is due to the oxidation of aromatics (41 %). While the ozonolysis of alkenes contributes to the formation of HCHO, some CHOCHO is formed through the oxidation of NMHCs by NO_3 radicals. However, compared to the OH initiated oxidation of NMHCs, ozonolysis of alkenes and NO_3 initiated NMHCs degradations are of minor importance in terms of the total HCHO and CHOCHO production. The observation of OH radicals at night results in maximum HCHO and CHOCHO concentrations during early morning, which however is different from observations at other places around the world.

Compared to the measurements, the box model overestimates the HCHO and CHOCHO concentrations by a factor of 2–5. This discrepancy seems to be caused by a combination of effects each contributing approximately by the same amount, i.e., the lack of knowledge about (1) fresh emissions, (2) fast vertical transport of precursor NMHCs, (3) dry deposition, (4) vertical dilution during the lift of the mixing layer height during early morning hours, and (5) uptake of HCHO and CHOCHO by aerosols. Our analysis indicates that, in addition to chemical considerations, physical processes like transport, dilution, and dry deposition have to be well considered for any model predicting HCHO and CHOCHO concentrations.

Our model simulations indicate that the CHOCHO to HCHO ratio at the BG site is influenced not only by the NMHC composition but also by the concentration levels of OH and NO_x. Higher R_{GF} result from higher aromatic contributions to total NMHCs, from higher OH and NO_2 but lower NO concentrations. Moreover, processes like vertical transport/dilution, dry deposition, and uptake by aerosols can also influence the CHOCHO to HCHO ratio. The complex dependence of R_{GF} on NMHCs, OH, NO_x, and other physical / chemical processes makes it difficult to use R_{GF} as an indicator of anthropogenic or biogenic emissions.

The Supplement related to this article is available online at doi:10.5194/acp-14-12291-2014-supplement.

Acknowledgements. This work was supported by the Strategic Priority Research Program of the Chinese Academy of Sciences (XDB05010500) and the National Natural Science Foundation of China (21190052). The research was also supported by the Collaborative Innovation Center for Regional Environmental Quality.

The service charges for this open access publication have been covered by a Research Centre of the Helmholtz Association.

Edited by: S. C. Liu

References

Choi, W., Faloona, I. C., Bouvier-Brown, N. C., McKay, M., Goldstein, A. H., Mao, J., Brune, W. H., LaFranchi, B. W., Cohen, R. C., Wolfe, G. M., Thornton, J. A., Sonnenfroh, D. M., and Millet, D. B.: Observations of elevated formaldehyde over a forest canopy suggest missing sources from rapid oxidation of arboreal hydrocarbons, Atmos. Chem. Phys., 10, 8761–8781, doi:10.5194/acp-10-8761-2010, 2010.

DiGangi, J. P., Boyle, E. S., Karl, T., Harley, P., Turnipseed, A., Kim, S., Cantrell, C., Maudlin III, R. L., Zheng, W., Flocke, F., Hall, S. R., Ullmann, K., Nakashima, Y., Paul, J. B., Wolfe, G. M., Desai, A. R., Kajii, Y., Guenther, A., and Keutsch, F. N.: First direct measurements of formaldehyde flux via eddy covariance: implications for missing in-canopy formaldehyde sources, Atmos. Chem. Phys., 11, 10565–10578, doi:10.5194/acp-11-10565-2011, 2011.

DiGangi, J. P., Henry, S. B., Kammrath, A., Boyle, E. S., Kaser, L., Schnitzhofer, R., Graus, M., Turnipseed, A., Park, J.-H., Weber, R. J., Hornbrook, R. S., Cantrell, C. A., Maudlin III, R. L., Kim, S., Nakashima, Y., Wolfe, G. M., Kajii, Y., Apel, E., Goldstein, A. H., Guenther, A., Karl, T., Hansel, A., and Keutsch, F. N.: Observations of glyoxal and formaldehyde as metrics for the anthropogenic impact on rural photochemistry, Atmos. Chem. Phys., 12, 9529–9543, doi:10.5194/acp-12-9529-2012, 2012.

Finlayson-Pitts, B. J. and Pitts, J. N.: Chemistry of the Upper and Lower Atmosphere - Theory, Experiments and Applications, Academic Press, San Diego, first edn., 2000.

Fortems-Cheiney, A., Chevallier, F., Pison, I., Bousquet, P., Saunois, M., Szopa, S., Cressot, C., Kurosu, T. P., Chance, K., and Fried, A.: The formaldehyde budget as seen by a global-scale multi-constraint and multi-species inversion system, Atmos. Chem. Phys., 12, 6699–6721, doi:10.5194/acp-12-6699-2012, 2012.

Fried, A., Crawford, J., Olson, J., Walega, J., Potter, W., Wert, B., Jordan, C., Anderson, B., Shetter, R., Lefer, B., Blake, D., Blake, N., Meinardi, S., Heikes, B., O'Sullivan, D., Snow, J., Fuelberg, H., Kiley, C. M., Sandholm, S., Tan, D., Sachse, G., Singh, H., Faloona, I., Harward, C. N., and Carmichael, G. R.: Airborne tunable diode laser measurements of formaldehyde during TRACE-P: Distributions and box model comparisons, J. Geophys. Res., 108, 8798, doi:10.1029/2003jd003451, 2003a.

Fried, A., Wang, Y., Cantrell, C., Wert, B., Walega, J., Ridley, B., Atlas, E., Shetter, R., Lefer, B., Coffey, M. T., Hannigan, J., Blake, D., Blake, N., Meinardi, S., Talbot, B., Dibb, J., Scheuer, E., Wingenter, O., Snow, J., Heikes, B., and Ehhalt, D.: Tunable

diode laser measurements of formaldehyde during the TOPSE 2000 study: Distributions, trends, and model comparisons, J. Geophys. Res., 108, D4, 8365, doi:10.1029/2002jd002208, 2003b.

Fried, A., Cantrell, C., Olson, J., Crawford, J. H., Weibring, P., Walega, J., Richter, D., Junkermann, W., Volkamer, R., Sinreich, R., Heikes, B. G., O'Sullivan, D., Blake, D. R., Blake, N., Meinardi, S., Apel, E., Weinheimer, A., Knapp, D., Perring, A., Cohen, R. C., Fuelberg, H., Shetter, R. E., Hall, S. R., Ullmann, K., Brune, W. H., Mao, J., Ren, X., Huey, L. G., Singh, H. B., Hair, J. W., Riemer, D., Diskin, G., and Sachse, G.: Detailed comparisons of airborne formaldehyde measurements with box models during the 2006 INTEX-B and MILAGRO campaigns: potential evidence for significant impacts of unmeasured and multigeneration volatile organic carbon compounds, Atmos. Chem. Phys., 11, 11867–11894, doi:10.5194/acp-11-11867-2011, 2011.

Fu, T.-M., Jacob, D. J., Wittrock, F., Burrows, J. P., Vrekoussis, M., and Henze, D. K.: Global budgets of atmospheric glyoxal and methylglyoxal, and implications for formation of secondary organic aerosols, J. Geophys. Res., 113, D15303, doi:10.1029/2007JD009505, 2008.

Garcia, A. R., Volkamer, R., Molina, L. T., Molina, M. J., Samuelson, J., Mellqvist, J., Galle, B., Herndon, S. C., and Kolb, C. E.: Separation of emitted and photochemical formaldehyde in Mexico City using a statistical analysis and a new pair of gas-phase tracers, Atmos. Chem. Phys., 6, 4545–4557, doi:10.5194/acp-6-4545-2006, 2006.

Hofzumahaus, A., Rohrer, F., Lu, K., Bohn, B., Brauers, T., Chang, C.-C., Fuchs, H., Holland, F., Kita, K., Kondo, Y., Li, X., Lou, S., Shao, M., Zeng, L., Wahner, A., and Zhang, Y.: Amplified Trace Gas Removal in the Troposphere, Science, 324, 1702–1704, doi:10.1126/science.1164566, 2009.

Hu, W. W., Hu, M., Deng, Z. Q., Xiao, R., Kondo, Y., Takegawa, N., Zhao, Y. J., Guo, S., and Zhang, Y. H.: The characteristics and origins of carbonaceous aerosol at a rural site of PRD in summer of 2006, Atmos. Chem. Phys., 12, 1811–1822, doi:10.5194/acp-12-1811-2012, 2012.

Huisman, A. J., Hottle, J. R., Galloway, M. M., DiGangi, J. P., Coens, K. L., Choi, W., Faloona, I. C., Gilman, J. B., Kuster, W. C., de Gouw, J., Bouvier-Brown, N. C., Goldstein, A. H., LaFranchi, B. W., Cohen, R. C., Wolfe, G. M., Thornton, J. A., Docherty, K. S., Farmer, D. K., Cubison, M. J., Jimenez, J. L., Mao, J., Brune, W. H., and Keutsch, F. N.: Photochemical modeling of glyoxal at a rural site: observations and analysis from BEARPEX 2007, Atmos. Chem. Phys., 11, 8883–8897, doi:10.5194/acp-11-8883-2011, 2011.

Jang, M. and Kamens, R. M.: Atmospheric Secondary Aerosol Formation by Heterogeneous Reactions of Aldehydes in the Presence of a Sulfuric Acid Aerosol Catalyst, Environ. Sci. Technol., 35, 4758–4766, doi:10.1021/es010790s, 2001.

Jayne, J. T., Worsnop, D. R., Kolb, C. E., Swartz, E., and Davidovits, P.: Uptake of Gas-Phase Formaldehyde by Aqueous Acid Surfaces, J. Phys. Chem., 100, 8015–8022, doi:10.1021/jp953196b, 1996.

Kormann, R., Fischer, H., de Reus, M., Lawrence, M., Brühl, C., von Kuhlmann, R., Holzinger, R., Williams, J., Lelieveld, J., Warneke, C., de Gouw, J., Heland, J., Ziereis, H., and Schlager, H.: Formaldehyde over the eastern Mediterranean during MINOS: Comparison of airborne in-situ measurements with 3D-model results, Atmos. Chem. Phys., 3, 851–861, doi:10.5194/acp-3-851-2003, 2003.

Kroll, J. H., Ng, N. L., Murphy, S. M., Varutbangkul, V., Flagan, R. C., and Seinfeld, J. H.: Chamber studies of secondary organic aerosol growth by reactive uptake of simple carbonyl compounds, J. Geophys. Res., 110, D23 207, doi:10.1029/2005jd006004, 2005.

Lee, M., Heikes, B. G., Jacob, D. J., Sachse, G., and Anderson, B.: Hydrogen peroxide, organic hydroperoxide, and formaldehyde as primary pollutants from biomass burning, J. Geophys. Res., 102, 1301–1309, doi:10.1029/96jd01709, 1997.

Li, X., Brauers, T., Shao, M., Garland, R. M., Wagner, T., Deutschmann, T., and Wahner, A.: MAX-DOAS measurements in southern China: retrieval of aerosol extinctions and validation using ground-based in-situ data, Atmos. Chem. Phys., 10, 2079–2089, doi:10.5194/acp-10-2079-2010, 2010.

Li, X., Brauers, T., Häseler, R., Bohn, B., Fuchs, H., Hofzumahaus, A., Holland, F., Lou, S., Lu, K. D., Rohrer, F., Hu, M., Zeng, L. M., Zhang, Y. H., Garland, R. M., Su, H., Nowak, A., Wiedensohler, A., Takegawa, N., Shao, M., and Wahner, A.: Exploring the atmospheric chemistry of nitrous acid (HONO) at a rural site in Southern China, Atmos. Chem. Phys., 12, 1497–1513, doi:10.5194/acp-12-1497-2012, 2012.

Li, X., Brauers, T., Hofzumahaus, A., Lu, K., Li, Y. P., Shao, M., Wagner, T., and Wahner, A.: MAX-DOAS measurements of NO2, HCHO and CHOCHO at a rural site in Southern China, Atmos. Chem. Phys., 13, 2133–2151, doi:10.5194/acp-13-2133-2013, 2013.

Li, Z., Schwier, A. N., Sareen, N., and McNeill, V. F.: Reactive processing of formaldehyde and acetaldehyde in aqueous aerosol mimics: surface tension depression and secondary organic products, Atmos. Chem. Phys., 11, 11 617–11 629, doi:10.5194/acp-11-11617-2011, 2011.

Liggio, J., Li, S.-M., and McLaren, R.: Reactive uptake of glyoxal by particulate matter, J. Geophys. Res., 110, D10 304, doi:10.1029/2004jd005113, 2005.

Liu, X., Cheng, Y., Zhang, Y., Jung, J., Sugimoto, N., Chang, S.-Y., Kim, Y. J., Fan, S., and Zeng, L.: Influences of relative humidity and particle chemical composition on aerosol scattering properties during the 2006 PRD campaign, Atmos. Environ., 42, 1525–1536, doi:10.1016/j.atmosenv.2007.10.077, 2008.

Liu, Z., Wang, Y., Vrekoussis, M., Richter, A., Wittrock, F., Burrows, J. P., Shao, M., Chang, C.-C., Liu, S.-C., Wang, H., and Chen, C.: Exploring the missing source of glyoxal (CHOCHO) over China, Geophys. Res. Lett., 39, L10812–, doi:10.1029/2012GL051645, 2012.

Lou, S., Holland, F., Rohrer, F., Lu, K., Bohn, B., Brauers, T., Chang, C. C., Fuchs, H., Häseler, R., Kita, K., Kondo, Y., Li, X., Shao, M., Zeng, L., Wahner, A., Zhang, Y., Wang, W., and Hofzumahaus, A.: Atmospheric OH reactivities in the Pearl River Delta – China in summer 2006: measurement and model results, Atmos. Chem. Phys., 10, 11243–11260, doi:10.5194/acp-10-11243-2010, 2010.

Lu, K. D., Rohrer, F., Holland, F., Fuchs, H., Bohn, B., Brauers, T., Chang, C. C., Häseler, R., Hu, M., Kita, K., Kondo, Y., Li, X., Lou, S. R., Nehr, S., Shao, M., Zeng, L. M., Wahner, A., Zhang, Y. H., and Hofzumahaus, A.: Observation and modelling of OH and HO2 concentrations in the Pearl River Delta 2006: a missing

OH source in a VOC rich atmosphere, Atmos. Chem. Phys., 12, 1541–1569, doi:10.5194/acp-12-1541-2012, 2012.

MacDonald, S. M., Oetjen, H., Mahajan, A. S., Whalley, L. K., Edwards, P. M., Heard, D. E., Jones, C. E., and Plane, J. M. C.: DOAS measurements of formaldehyde and glyoxal above a south-east Asian tropical rainforest, Atmos. Chem. Phys., 12, 5949–5962, doi:10.5194/acp-12-5949-2012, 2012.

Myriokefalitakis, S., Vrekoussis, M., Tsigaridis, K., Wittrock, F., Richter, A., Brühl, C., Volkamer, R., Burrows, J. P., and Kanakidou, M.: The influence of natural and anthropogenic secondary sources on the glyoxal global distribution, Atmos. Chem. Phys., 8, 4965–4981, doi:10.5194/acp-8-4965-2008, 2008.

Parrish, D. D., Ryerson, T. B., Mellqvist, J., Johansson, J., Fried, A., Richter, D., Walega, J. G., Washenfelder, R. A., de Gouw, J. A., Peischl, J., Aikin, K. C., McKeen, S. A., Frost, G. J., Fehsenfeld, F. C., and Herndon, S. C.: Primary and secondary sources of formaldehyde in urban atmospheres: Houston Texas region, Atmos. Chem. Phys., 12, 3273–3288, doi:10.5194/acp-12-3273-2012, 2012.

Sassine, M., Burel, L., D'Anna, B., and George, C.: Kinetics of the tropospheric formaldehyde loss onto mineral dust and urban surfaces, Atmos. Environ., 44, 5468–5475, doi:10.1016/j.atmosenv.2009.07.044, 2010.

Schauer, J. J., Kleeman, M. J., Cass, G. R., and Simoneit, B. R. T.: Measurement of Emissions from Air Pollution Sources. 2. C1 through C30 Organic Compounds from Medium Duty Diesel Trucks, Environ. Sci. Technol., 33, 1578–1587, doi:10.1021/es980081n, 1999.

Schauer, J. J., Kleeman, M. J., Cass, G. R., and Simoneit, B. R. T.: Measurement of Emissions from Air Pollution Sources. 5. C1 through C32 Organic Compounds from Gasoline-Powered Motor Vehicles, Environ. Sci. Technol., 36, 1169–1180, doi:10.1021/es0108077, 2002.

Stavrakou, T., Müller, J. F., De Smedt, I., Van Roozendael, M., Kanakidou, M., Vrekoussis, M., Wittrock, F., Richter, A., and Burrows, J. P.: The continental source of glyoxal estimated by the synergistic use of spaceborne measurements and inverse modelling, Atmos. Chem. Phys., 9, 8431–8446, doi:10.5194/acp-9-8431-2009, 2009.

Stickler, A., Fischer, H., Williams, J., de Reus, M., Sander, R., Lawrence, M. G., Crowley, J. N., and Lelieveld, J.: Influence of summertime deep convection on formaldehyde in the middle and upper troposphere over Europe, J. Geophys. Res., 111, D14308, doi:10.1029/2005jd007001, 2006.

Stull, R. B.: An Introduction to Boundary Layer Meteorology, Kluwer Academic Publishers, Dordrecht, The Netherlands, 1988.

Tan, Y., Perri, M. J., Seitzinger, S. P., and Turpin, B. J.: Effects of Precursor Concentration and Acidic Sulfate in Aqueous Glyoxal-OH Radical Oxidation and Implications for Secondary Organic Aerosol, Environ. Sci. Technol., 43, 8105–8112, doi:10.1021/es901742f, 2009.

Tie, X., Brasseur, G., Emmons, L., Horowitz, L., and Kinnison, D.: Effects of aerosols on tropospheric oxidants: A global model study, J. Geophys. Res., 106, 22931–22964, doi:10.1029/2001jd900206, 2001.

Toda, K., Yunoki, S., Yanaga, A., Takeuchi, M., Ohira, S.-I., and Dasgupta, P. K.: Formaldehyde Content of Atmospheric Aerosol, Environ. Sci. Technol., 48, 6636–6643, doi:10.1021/es500590e, 2014.

Volkamer, R., San Martini, F., Molina, L. T., Salcedo, D., Jimenez, J. L., and Molina, M. J.: A missing sink for gas-phase glyoxal in Mexico City: Formation of secondary organic aerosol, Geophys. Res. Lett., 34, L19807, doi:10.1029/2007gl030752, 2007.

Volkamer, R., Sheehy, P., Molina, L. T., and Molina, M. J.: Oxidative capacity of the Mexico City atmosphere – Part 1: A radical source perspective, Atmos. Chem. Phys., 10, 6969–6991, doi:10.5194/acp-10-6969-2010, 2010.

Vrekoussis, M., Wittrock, F., Richter, A., and Burrows, J. P.: GOME-2 observations of oxygenated VOCs: what can we learn from the ratio glyoxal to formaldehyde on a global scale?, Atmos. Chem. Phys., 10, 10145–10160, doi:10.5194/acp-10-10145-2010, 2010.

Wagner, V., Schiller, C., and Fischer, H.: Formaldehyde measurements in the marine boundary layer of the Indian Ocean during the 1999 INDOEX cruise of the R/V Ronald H. Brown, J. Geophys. Res., 106, 28529–28538, doi:10.1029/2000jd900825, 2001.

Wang, X., Gao, S., Yang, X., Chen, H., Chen, J., Zhuang, G., Surratt, J. D., Chan, M. N., and Seinfeld, J. H.: Evidence for High Molecular Weight Nitrogen-Containing Organic Salts in Urban Aerosols, Environ. Sci. Technol., 44, 4441–4446, doi:10.1021/es1001117, 2010.

Washenfelder, R. A., Young, C. J., Brown, S. S., Angevine, W. M., Atlas, E. L., Blake, D. R., Bon, D. M., Cubison, M. J., de Gouw, J. A., Dusanter, S., Flynn, J., Gilman, J. B., Graus, M., Griffith, S., Grossberg, N., Hayes, P. L., Jimenez, J. L., Kuster, W. C., Lefer, B. L., Pollack, I. B., Ryerson, T. B., Stark, H., Stevens, P. S., and Trainer, M. K.: The glyoxal budget and its contribution to organic aerosol for Los Angeles, California, during CalNex 2010, J. Geophys. Res., 116, D00V02, doi:10.1029/2011JD016314, 2011.

Wittrock, F., Richter, A., Oetjen, H., Burrows, J. P., Kanakidou, M., Myriokefalitakis, S., Volkamer, R., Beirle, S., Platt, U., and Wagner, T.: Simultaneous global observations of glyoxal and formaldehyde from space, Geophys. Res. Lett., 33, L16804, doi:10.1029/2006gl026310, 2006.

Zhang, Q., Jimenez, J. L., Worsnop, D. R., and Canagaratna, M.: A Case Study of Urban Particle Acidity and Its Influence on Secondary Organic Aerosol, Environ. Sci. Technol., 41, 3213–3219, doi:10.1021/es061812j, 2007.

Zhou, X., Lee, Y.-N., Newman, L., Chen, X., and Mopper, K.: Tropospheric formaldehyde concentration at the Mauna Loa Observatory during the Mauna Loa Observatory Photochemistry Experiment 2, J. Geophys. Res., 101, 14711–14719, doi:10.1029/95jd03226, 1996.